Journal of Alloys and Compounds 909 (2022) 164821

Contents lists available at ScienceDirect

Journal of Alloys and Compounds

journal homepage: www.elsevier.com/locate/jalcom

Antiferromagnetic resonance and magnetic anisotropy in $Pr_xY_{1-x}Fe_3(BO_3)_4$ crystals in the region of the magnetic structure transformation "easy axis – easy plane"

A.I. Pankrats[a,b,*], S.M. Zharkov[a,b], G.M. Zeer[b], I.A. Gudim[a]

[a] Kirensky Institute of Physics, Federal Research Center KSC SB RAS, Akademgorodok 50/38, Krasnoyarsk 660036, Russia
[b] Siberian Federal University, 79 Svobodny st., Krasnoyarsk 660041, Russia

ARTICLE INFO

Article history:
Received 18 February 2022
Received in revised form 21 March 2022
Accepted 28 March 2022
Available online 30 March 2022

Keywords:
Magnetically ordered materials
Rare earth alloys and compounds
Spin dynamics
Anisotropy
Magnetic measurements
Scanning electron microscopy, SEM

ABSTRACT

The spin dynamics, magnetic structures and magnetic anisotropy of single crystals $Pr_xY_{1-x}Fe_3(BO_3)_4$ have been studied using antiferromagnetic resonance (AFMR) in a wide range of frequencies, magnetic fields, and temperatures. The frequency-field dependences of AFMR for the crystals with x = 0.25 and 0.45 are characteristic of antiferromagnets with the easy plane (EP) anisotropy. The crystals with x = 0.75 and 1.0 exhibit frequency-field dependences that are typical for antiferromagnets with the easy axis (EA) anisotropy. In these crystals, a significant decrease in the effective anisotropy fields of praseodymium upon the transition to the spin-flop state has been found. It is shown that this is the main reason for the large lability intervals, within which the regions of coexistence of the collinear and spin-flop states overlap. In the crystal with x = 0.67, the magnetic field applied along the trigonal axis of the crystal leads to the spin reorientation transition from the EA to the EP state. A magnetic phase diagram of the states on the plane "magnetic field - temperature" is built. In this crystal, the effective anisotropy field of praseodymium also decreases upon the transition to the field-induced EP state. Diamagnetic dilution of the praseodymium subsystem leads to the contribution of this subsystem to the total anisotropy field depending almost linearly on the praseodymium concentration.

1. Introduction

In the last two decades rare-earth (RE) ferroborates $RM_3(BO_3)_4$ (R = Y, La–Lu; M = Fe, Cr, Al, Ga) have attracted serious attention of researchers in the area of solid state physics. These compounds crystallize in the non-centrosymmetric trigonal space group *R*32; upon cooling, in the compounds with lower ionic radius values of RE ions (R = Eu, Gd, Tb, Dy, Ho, Er) there occurs a structural transition into $P3_121$ with the transition temperature linearly dependent on the ionic radius of RE ions [1,2]. The initial interest to these materials appeared due to the possibilities of using them with diamagnetic ions in the M-position in non-linear optics and solid state lasers [3–5]. Later, a number of crystals of this family were found to be multiferroics with the coexistence of the interconnected magnetic, electric and elastic order parameters [see, e.g., [6–8].

This family of crystals is of special interest due to the study of its magnetic properties. This research interest is caused by the fact that the presence of two interconnected magnetic subsystems (3d and 4f ions) in the crystals results in a great variety of magnetic structures and phase transitions between them. The study of the magnetic properties of yttrium ferroborate $YFe_3(BO_3)_4$, containing only the iron magnetic subsystem [8–10], shows that this antiferromagnetically ordered subsystem is characterized by the easy plane (EP) type anisotropy with the magnetic moments of Fe^{3+}ions parallel to the basal plane of the crystal. In RE crystals this subsystem has a polarizing impact on the RE subsystem; as a result, the latter makes an additional contribution into the total crystal anisotropy. Depending on the value and sign of the magnetic anisotropy of the RE subsystem, the resulting magnetic structure with the easy axis (EA) or EP magnetic anisotropy is formed in the crystal. As is shown by the results of the elastic neutron scattering and magnetic X-ray scattering, some of the magnetic structures can be weakly non-collinear (R=Ho [9] and Er [11]) or incommensurate ones (R = Nd [12] and Gd above 10 K [13]). In Gd and Ho ferroborates, the contributions of the RE and iron subsystems to the total anisotropy

* Corresponding author at: Kirensky Institute of Physics, Federal Research Center KSC SB RAS, Akademgorodok 50/38, Krasnoyarsk 660036, Russia
E-mail address: pank@iph.krasn.ru (A.I. Pankrats).

https://doi.org/10.1016/j.jallcom.2022.164821
0925-8388/

have close absolute values but opposite signs and are competing. Due to the different temperature dependences of these contributions, the total anisotropy field changes its sign at a certain temperature and a spontaneous spin reorientation transition between the EA and EP magnetic structures occurs [9,13–15].

There are several possibilities of regulating the total magnetic anisotropy in the family of RE ferroborates. One of them is to change the RE contribution into the anisotropy by mixing the contribution of different RE ions [16–18]. The ratio of the contributions of the RE and Fe subsystems can also change upon the diamagnetic dilution of one of the subsystems. For example, the diamagnetic dilution of the iron subsystem in $GdFe_3(BO_3)_4$ by Ga^{3+} ions results in the fact that the crystal $GdFe_{2.1}Ga_{0.9}(BO_3)_4$ shows the EA anisotropy in the whole temperature region of the magnetic order [19]. On the other hand, the diamagnetic dilution of the gadolinium subsystem in this crystal decreases the contribution of the Gd^{3+} subsystem; as a result, the $Gd_{1-x}Y_xFe_3(BO_3)_4$ crystal is characterized by the EP magnetic anisotropy in the whole region below the Nel temperature [10].

A similar effect of the diamagnetic dilution of the RE subsystem is observed in the crystals $Pr_xY_{1-x}Fe_3(BO_3)_4$. In the pure $PrFe_3(BO_3)_4$ the EA contribution of the Pr^{3+} ion subsystem to the total magnetic anisotropy prevails and determines the EA antiferromagnetic structure of the crystal in the whole temperature region of the magnetic order below the Néel temperature T_N = 32 K [11,20]. The study using high resolution neutron powder diffraction [21], as well as the temperature and field dependences of magnetization [22] showed that, as a result of the competing magnetic anisotropy contribution of the subsystems, the transition from the EA antiferromagnetic structure to the EP one occurs in these crystals through the formation of inclined magnetic structures in the region of the praseodymium concentration x = 0.45÷0.67. Moreover, the angle between the basal plane and antiferromagnetic vector of the iron subsystem monotonously grows in this region with an increase in x. In [22] a theoretical description was also presented for the experimental results of the magnetostatic investigations based on the approximation of the molecular field for Fe^{3+} ions and on the crystal field model for RE ions. During the investigation of the field dependences of the magnetization of the crystals with x = 0.75 and 0.67 in the magnetic field applied along the ***c***-axis, unusual spin reorientations with a two-step jump of the magnetization were found. In [22] this effect was explained by the fact that within a certain range of magnetic fields between the first and second steps, an interjacent inclined phase is formed with the tilt angle of the antiferromagnetic vector different from the corresponding tilt angle in the initial state without the magnetic field.

The method of antiferromagnetic resonance (AFMR) is very sensitive to the magnetic structure of a crystal. Antiferromagnetic crystals with different types of crystal symmetry (cubic, uniaxial, rhombic, etc.) show different shapes of the frequency-field dependences of AFMR. In addition, such dependences are qualitatively different for antiferromagnetic crystals that belong to the same type of the crystal symmetry, for example, uniaxial, but are characterized by different types of the magnetic anisotropy - EA or EP. As opposed to powder neutron diffraction, AFMR allows investigating the transformation of the magnetic structure upon changing the external magnetic field. Another advantage of the method is the ability to study magnetic anisotropy (and some other interactions in crystals), since the corresponding effective fields determine the resonant frequencies of AFMR.

The present study is devoted to the investigation of spin dynamics, magnetic structures and magnetic anisotropy of single crystals of $Pr_xY_{1-x}Fe_3(BO_3)_4$ as a function of temperature and magnetic fields using the AFMR method. Of special interest are the resonant properties in the area of concentrations where there occurs the active transformation from the EP to EA magnetic structure, and inclined magnetic structures are formed. For the samples with x = 0.75÷1 showing the EA anisotropy, we have found large lability intervals in the region of the spin-flop transition. These intervals increase in the course of the diamagnetic dilution of the praseodymium subsystem. In the crystal with x = 0.67 with the EA ground state it is found that upon reaching the critical magnetic field applied along the ***c***-axis, the sign of the total anisotropy of the crystal changes, which induces the spin reorientation transition into the EP structure.

2. Experimental details

2.1. Sample preparation

Single crystals were grown from fluxes based on trimolibdate bismuth (100 – n) wt% {$Bi_2Mo_3O_{12}$ + $3B_2O_3$ + 0.5[xPr_2O_3 + (1–x) Y_2O_3]} + n wt% $Pr_xY_{1-x}Fe_3(BO_3)_4$; the procedure of single crystal growth is described in [23]. For the concentration n = 20, the saturation temperature was $T_s \approx 950^0$ C and its concentration dependence can be described as $dT_s/dn \approx 6^0$ C/wt%. The crystals were grown on seeds at a starting temperature $T = T_s - 7^0$ C with the subsequent decrease in the temperature by 1^0 C/day for 5 days. Single crystals of about 4–6 mm in size were grown.

2.2. Resonance measurements

The AFMR study of the $Pr_xY_{1-x}Fe_3(BO_3)_4$ single crystals was carried out on an original magnetic resonance spectrometer with the broad frequency band (25–140 GHz) and pulsed magnetic fields of up to 90 kOe [24]. A few measurements were carried out using a spectrometer with a superconducting magnetic solenoid, with the sample being placed into a cylindrical resonator with the H_{01n} mode tuned within the range of 25÷80 GHz with n = 1÷3.

2.3. SEM and EDS characterization

The microstructure and local elemental composition of the $Pr_xY_{1-x}Fe_3(BO_3)_4$ samples were investigated using scanning electron microscopy (SEM) and energy dispersive X-ray spectroscopy (EDS). The SEM and EDS experiments were performed with JEOL JSM-7001 F equipped with an energy dispersive X-ray spectrometer (Oxford Instruments INCA PentaFETx3).

3. Experimental results and discussion

3.1. AFMR in $YFe_3(BO_3)_4$ and $PrFe_3(BO_3)_4$

The spin dynamics of unsubstituted edge compounds of $Pr_xY_{1-x}Fe_3(BO_3)_4$ family was partly investigated earlier. The frequency-field, angular and temperature dependences of AFMR in the single crystal $YFe_3(BO_3)_4$ [10], whose magnetic structure is determined only by the subsystem of iron ions, confirms the formation of the antiferromagnetic EP structure in this subsystem within the whole temperature range below the Néel temperature T_N = 38 K. For the magnetic field applied along the trigonal axis, the gap in the AFMR spectrum was measured which at T= 4.2 K is equal to $\nu_{c\|}$= 124 GHz. The experimental temperature dependence of the gap along the whole temperature range of the magnetic ordering is well described by the Brillouin function for the spin S= 5/2, which characterizes the temperature dependence of the iron sublattice magnetization $m(T)$. Since the value of the gap $\nu_{c\|} = \gamma_{\|}\sqrt{2H_E\left|H_A^{Fe}\right|}$ is determined by the effective fields of the magnetic anisotropy of the iron subsystem H_A^{Fe} and exchange H_E, this temperature dependence of the gap evidences that both effective magnetic fields are proportional to $m(T)$. Based on this dependence, in [10] a conclusion is

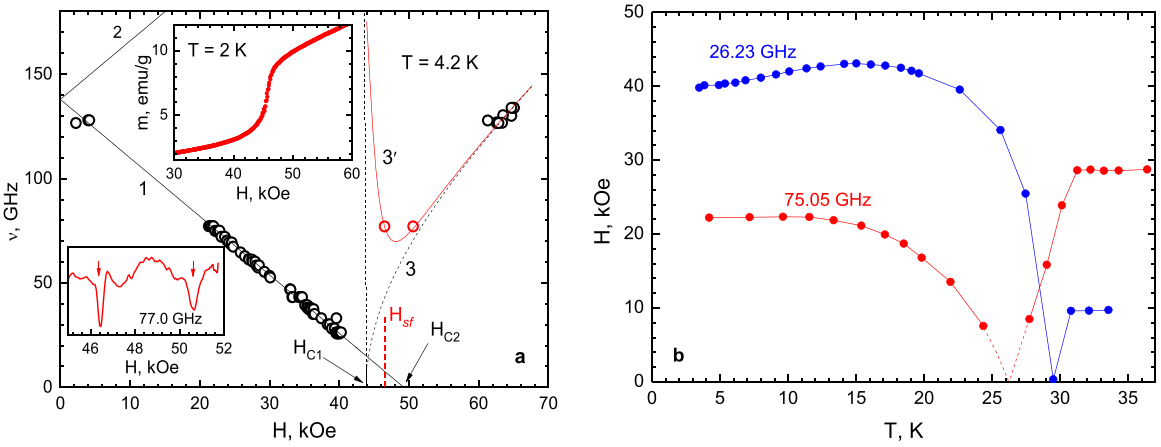

Fig. 1. a - frequency-field dependence of AFMR in $PrFe_3(BO_3)_4$ at T = 4.2 K, **H**||***c***; in the insets: top –the spin-flop transition measured at T = 2 K, bottom - AFMR spectrum in the region of the spin-flop transition measured at a frequency of 77,0 GHz; b - temperature dependence of the resonance fields at frequencies of 26.23 and 75.05 GHz.

made that the magnetic anisotropy in yttrium ferroborate is mainly determined by a pair mechanism (anisotropic exchange and/or dipolar interaction).

The AFMR investigation results regarding the EA antiferromagnet $PrFe_3(BO_3)_4$ were first presented in [25], where the energy gap in the AFMR spectrum and its temperature dependence were determined.

Our preliminary results on studying the frequency-field dependences of AFMR in $PrFe_3(BO_3)_4$ at T = 4.2 K were first presented in [22], and, subsequently, at the same temperature, by Bludov et al. in [26]. Since none of the above papers considered the frequency-field dependences of AFMR in $PrFe_3(BO_3)_4$ in a temperature range, the experimental frequency-field and temperature dependences of AFMR for this crystal will be presented below.

Fig. 1a shows the frequency-field dependence of AFMR in $PrFe_3(BO_3)_4$, measured at T = 4.2 K in the magnetic field oriented along the trigonal axis, **H**||***c***. In this dependence, two regions can be clearly distinguished. In the region of small magnetic fields there are two branches of oscillations (1 and 2), whose frequencies in the model of the collinear two-sublattice antiferromagnet with the EA anisotropy linearly depend on the applied magnetic field H [27,28]:

$$\frac{\nu_{1,2}}{\gamma_{||}} = [(2H_E + H_A)H_A + (\alpha H/2)^2]^{1/2} \pm H(1 - \alpha/2),$$
$$H < H_{sf} = \sqrt{(2H_E - H_A)H_A},\ \alpha = \chi_{||}/\chi_{\perp},\ H_{\Delta} = \sqrt{(2H_E + H_A)H_A} \equiv H_{C2}, \quad (1)$$

where H_{sf} is the critical field of the spin-flop transition, H_{C2} is the field of softening of the branch ν_1, $\chi_{||}$ and $\chi_{\perp}$ are the magnetic susceptibilities in the direction of the trigonal axis and in the basal plane, respectively. In this field range and in the frequency range covered by the spectrometer, only the branch ν_1 is observed which is a descending branch of AFMR (the sign "-" in the formula for $\nu_{1,2}$). The frequency-field dependence is well described by Eq. (1) with the gap in the AFMR spectrum $\nu_{c||} = \gamma_{||}H_{\Delta}$ = (138.0 ± 0.4) GHz and $\gamma_{||}$ = (2.80 ± 0.01) MHz/Oe, H_{C2} = 49.3 kOe. The parameters are close to the ones measured at T = 4.2 K in [26]. Theoretical dependences 1 and 2, shown in the Figure by the solid lines are built taking into account the obtained parameters. The measured value of the energy gap in the spectrum allows calculating the effective anisotropy field for $PrFe_3(BO_3)_4$ at T = 4.2 K H_A = 1.74 kOe, with the effective exchange field for the iron subsystem H_E = 700 kOe being used in the calculations [10]. It is clear that, in all the $Pr_xY_{1-x}Fe_3(BO_3)_4$ crystals with $x \neq 0$, the effective anisotropy field H_A is the total field involving the contributions of both praseodymium H_A^{Pr} and iron H_A^{Fe} subsystems. Their separation will be discussed in Section 4.

In the region of the spin-flop transition the resonance absorption is found only at frequencies higher than ~70 GHz. The bottom inset of Fig. 1 shows the AFMR spectrum recorded at T = 4.2 K at a frequency of 77.0 GHz using the spectrometer with a superconducting solenoid. The red arrows indicate the resonance absorption lines; on the frequency-field dependence, these lines are denoted by the red dots. In the spin-flop state at $H > H_{sf}$ with the magnetic field orientation **H**||***c*** there is an AFMR branch with the non-zero frequency [27]:

$$\left(\frac{\nu_1}{\gamma_{||}}\right)^2 \approx H^2 - H_{C1}^2,\ H > H_{sf},\ H_{C1} = \sqrt{\frac{(2H_E - H_A)^2 H_A}{2H_E + H_A}}, \quad (2)$$

where H_{C1} is the critical field which determines the lability interval $H_{C1} \div H_{C2}$, in which the collinear and spin-flop states coexist. In the Figure, dashed line 3 shows the frequency-field dependence built using Eq. (2) taking into account the critical field H_{C1} = 43.9 kOe. Note that the field of the spin-flop transition H_{sf} = 46.4 kOe, obtained from the field dependence of the magnetization [22] (see the top inset in Fig. 1) does not coincide with any of the critical fields H_{C1} or H_{C2} and lies within the lability interval $H_{C1} \div H_{C2}$. In the region of the spin-flop transition, the calculated dependence poorly describes the experimental points. Apparently, the reason for this is the imprecise orientation of the applied magnetic field relative to the trigonal axis of the crystal. To calculate the frequency-field dependence of AFMR, in this case, use was made of the program for the numeric calculation of AFMR at an arbitrary orientation of the magnetic field [29]. This program is based on a model similar to that used in the derivation of Eqs. (1) and (2). Solid red line 3′ shows the frequency-field dependence calculated for the angle between the magnetic field and the trigonal axis θ = 1.8°, which best describes the experimental points.

At the field orientation **H**⊥***c*** the resonant properties were not studied since, in this case, the resonance frequencies at T = 4.2 K are outside the frequency range of the spectrometer.

The temperature dependences of the resonance fields **H**||***c*** measured at two frequencies are presented in Fig. 1b. Both dependences have a specific shape due to the fact that at low temperatures the resonance absorption corresponds to descending branch 1 of the frequency-field dependence (Fig. 1a). The dependence attenuation corresponds to the temperature at which the energy gap is equal to the measurement frequency; upon a further temperature increase the resonance absorption corresponds to the ascending AFMR branch 2.

The energy gap in the AFMR spectrum and effective field of anisotropy for $PrFe_3(BO_3)_4$ are shown as the functions of temperature in Fig. 2a and b. To calculate the $H_{\Delta}(T)$ dependence, the temperature dependence of the resonance field at a frequency of 26.23 GHz and magnetic susceptibilities $\chi_{||}(T)$ and $\chi_{\perp}(T)$ for the Fe subsystem [20] were used. Here, as in the case with $YFe_3(BO_3)_4$ [10], the temperature

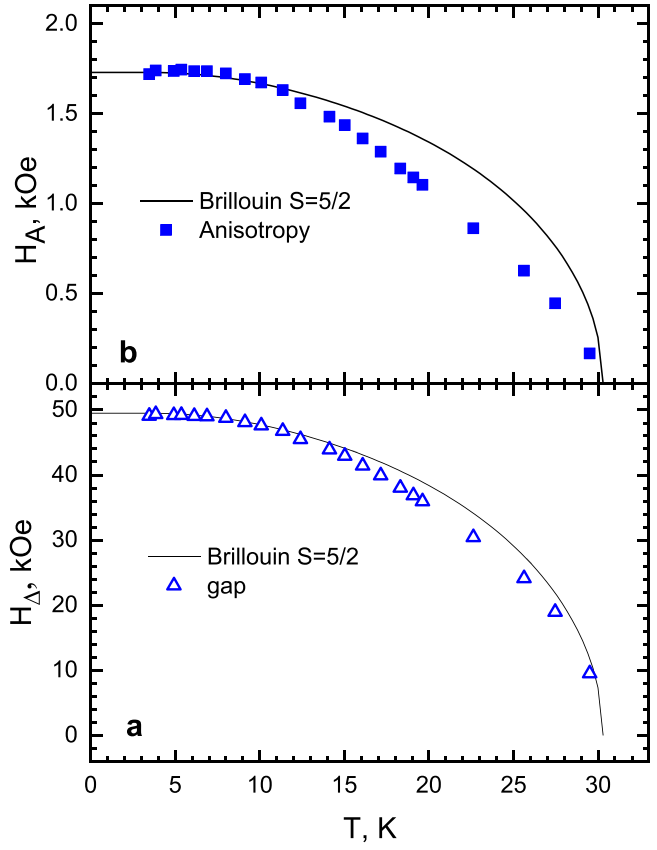

Fig. 2. Temperature dependences of the gap in the AFMR spectrum (a) and of the effective field of the magnetic anisotropy (b) for the single crystal of $PrFe_3(BO_3)_4$.

dependent exchange field which is needed to calculate $H_A(T)$ was considered to be determined by the magnetization of the iron ion sublattice $m^{Fe}(T)$. However, one can expect that in contrast to $YFe_3(BO_3)_4$, the m^{Fe} vs. T dependence in $PrFe_3(BO_3)_4$ might be a little different from the Brillouin function for S= 5/2. This difference is caused by the additional f-d exchange interaction between the Fe- and Pr-sublattices even if the total moment on the Pr-site amounts only to about 0.8 μ_B. Since any experimental data on $m^{Fe}(T)$ for $PrFe_3(BO_3)_4$ are unknown, we used neutron data on the temperature dependence of the magnetic moment values of the Fe-sublattice for the $Pr_{0.67}Y_{0.33}Fe_3(BO_3)_4$ crystal [21], which is close in the praseodymium content to the pure $PrFe_3(BO_3)_4$. As is expected, due to the dominating contribution of the praseodymium subsystem to the total anisotropy and the f-d exchange interaction, both $H_\Delta(T)$ and $H_A(T)$ dependences are poorly described by the Brillouin function for S= 5/2.

3.2. AFMR in the $Pr_xY_{1-x}Fe_3(BO_3)_4$ crystals with $x = 0.25$ and 0.45

For this group of crystals, neutron investigations were carried out only for x = 0.45 [21], the research results show that the magnetic structure of this crystal is close to the EP structure, which is characteristic for $YFe_3(BO_3)_4$, the magnetic moments of Fe^{3+} ions deviate from the basal plane only by the angle Θ^{Fe}= 16°. It is reasonable to assume that if in the sample with x = 0.25 an inclined magnetic structure is formed, then the magnetic moments deviate from the basal plane by the angle Θ^{Fe}, which is even smaller than for x = 0.45. The magnetic properties of both crystals including the magnetization as functions of the temperature and magnetic fields [22] were also characteristic for the EP magnetic structure.

This understanding of the magnetic structure of these crystals is confirmed by the AFMR investigations. The frequency-field dependences of AFMR for these two crystals measured at T= 4.2 K with the magnetic field orientation H||c and H⊥c, are shown in Fig. 3a and b. In both crystals in the magnetic field applied in the basal plane of the crystal, one can observe the gapless branch of AFMR which is typical for the EP state and whose frequency $\nu_{\perp 1}$ in the case of $H_A \ll H_E$ is proportional to the applied field (3) [27]:

$$\frac{\nu_{\perp 1}}{\gamma_\perp} = H_0\sqrt{1+\frac{|H_A|}{2H_E}} \approx H_0;\ \left(\frac{\nu_{\perp 2}}{\gamma_\perp}\right)^2 = 2H_E|H_A| - \frac{|H_A|}{2H_E}H_0^2 \quad (3)$$

The gyromagnetic ratio takes the values $\gamma_\perp$ = (2.80 ± 0.01) MHz/Oe for the crystal with x = 0.25 and $\gamma_\perp$ = (2.82 ± 0.01) MHz/Oe for x = 0.45.

It is difficult to observe the oscillations of the second branch in this orientation upon field scanning, since, as it follows from (3) for $\nu_{\perp 2}$, in the field range up to ~35 kOe the resonance frequency hardly depends on the magnetic field. The dashed lines show the frequency-field dependence for this branch of oscillations for both crystals. It is worth noting that in the crystal with x = 0.45 in the intersection region of the oscillation branches $\nu_{\perp 1}$ and $\nu_{\perp 2}$, additional lines are observed, indicated by the red and blue triangles in Fig. 3b. The presence of these lines and their specific frequency-field dependence indicate that in the intersection region of the modes $\nu_{\perp 1}$ and $\nu_{\perp 2}$ there occurs their interaction and formation of coupled oscillations with the characteristic entanglement and repulsion of branches. This type of formation of coupled oscillations at the intersection of the low-frequency and high-frequency modes was observed in antiferromagnets $MnCO_3$ [30] and α-Fe_2O_3 [31]. In these

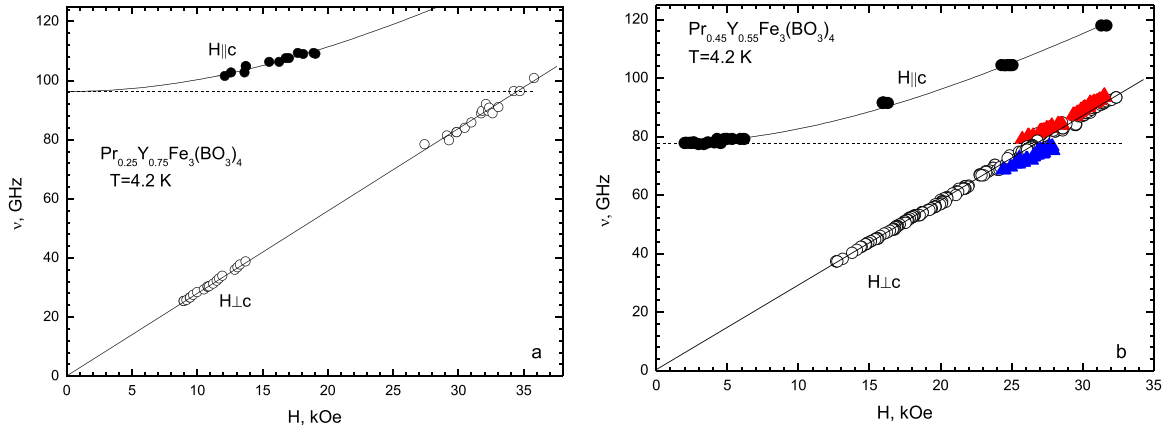

Fig. 3. Frequency-field dependences of AFMR in $Pr_xY_{1-x}Fe_3(BO_3)_4$ with x = 0.25 (a) and 0.45 (b) at T = 4.2 K, H||c and H⊥c.

Table 1
Gyromagnetic ratios γ, energy gaps H_Δ, total anisotropy fields H_A and anisotropy fields of praseodymium H_A^{Pr} [a)] for the $Pr_xY_{1-x}Fe_3(BO_3)_4$ single crystals at T = 4.2 K.

Content x in a charge	Content, x_{EDS}	γ, MHz/Oe	H_Δ, kOe	H_A, kOe	H_A^{Pr}, kOe	H_A^{Pr}, kOe $H > H_c$, H_{sf}
x = 0 $YFe_3(BO_3)_4$	–	2,80- H||c [10] 2,76 - H⊥c [10]	44.3 [10]	−1.44 [10]		
x = 0.25	0.27	2.80 ± 0.01 - H||c 2.80 ± 0.01 - H⊥c	34.4 ± 0.1	−0.84	0.56 ± 0.04	
x = 0.45	0.38	2.84 ± 0.02 - H||c 2.82 ± 0.01 - H⊥c	27.4 ± 0.2	−0.54	0.86 ± 0.04	
x = 0.67	0.60	2.83 ± 0.01 - H||c, H < H_c 2.83 ± 0.02 - H||c, H > H_c	19.8 ± 0.1 11.1 ± 0.2	0.28 −0.09	1.68 ± 0.04	1.35
x = 0.75	0.67	2.85–2.88 - H||c	26,9 ± 0.1	0.52	1.92 ± 0.04	1.50
x = 0.83 [b)]	0.74	2.85–2.88 - H||c	33,2 ± 0.1	0.83	2.23 ± 0.04	1.74
x = 1.0 $PrFe_3(BO_3)_4$	–	2.80 ± 0.01- H||c	49.3 ± 0.1	1.74	3.14 ± 0.04	2.82

[a)] – the calculation of the anisotropy fields of the Pr-subsystem will be discussed in Section 4.
[b)] – data in the crystal with x = 0.75 for the area with the greater praseodymium content (See the comments in Section 3.4); the value was recalculated from the real x_{EDS} for this area, taking into account the relation x_{EDS}/x_{charge} = 0.89, obtained for x = 0.75.

studies, it is shown that in the EP antiferromagnets upon the precise orientation of the magnetic field in the basal plane, the oscillation modes do not interact with each other upon intersecting the resonance frequencies, and coupled oscillations are formed at small deviations of the magnetic field from the basal plane. Thus, in the crystal with x = 0.25, in which the magnetic structure is likely to be very close to that of the EP antiferromagnet, at H⊥*c* no peculiarities are observed on the frequency-field dependence for the low-frequency branch in the region of intersection with the high-frequency branch. However, in the crystal with x = 0.45 due to the formation of the inclined magnetic structure, and deviations of the antiferromagnetic vector from the basal plane, the oscillating modes appear to interact even at **H⊥*c***.

If the magnetic field is applied along the trigonal axis of the crystal, **H||*c***, then, in both crystals, one branch of oscillations is observed with the energy gap determined by the effective exchange and magnetic anisotropy fields [27]:

$$\left(\frac{\nu_{||}}{\gamma_{||}}\right)^2 = H_\Delta^2 + H_o^2,\ H_\Delta^2 = 2H_E|H_A| \qquad (4)$$

The theoretical dependences built according to this equation shown in solid lines in the Fig. 3a and b well describe the experimental data with the parameters given in Table 1.

In Fig. 4, the resonance fields for both crystals are given as functions of temperature. If the magnetic field is applied in the basal plane, then the resonance field is independent of the temperature, as it follows from (3). Upon reaching the Néel temperature T_N = 33.7 K, the antiferromagnetic order disappears and a paramagnetic state is established in the crystal. At temperatures above T_N, the resonant absorption corresponds to the electron paramagnetic resonance (EPR) whose frequency changes with the magnetic field, as $\nu = \gamma H$, which coincides with (3). This dependence, measured at a frequency of 94.26 GHz for the crystal with x = 0.25, is presented in Fig. 4. However, if the field is applied along the trigonal axis, the resonance field strongly depends on the temperature in the region of the magnetic ordering, forming a plateau upon reaching T_N. Eq. (4) allow one to calculate, based on the temperature evolutions of the resonance fields for both crystals for H||c, the temperature dependences of the energy gaps H_Δ of the AFMR spectrum and of the total effective anisotropy fields H_A. When calculating the anisotropy fields H_A at T = 4.2 K for both crystals, the value of the exchange field H_E = 700 kOe was used, which is considered independent of the substitution in the RE subsystem. To form the temperature variations of the exchange field, real neutron data on the magnetic moment of the Fe-sublattice $m^{Fe}(T)$ in the compound with x = 0.45 [21] were used. For the crystal with the minimal content of praseodymium x = 0.25, the Brillouin function for S = 5/2 can be a good approximation. The temperature dependences of the total anisotropy fields for both crystals along with the results for other crystals of this family are given in Fig. 5. As it is expected, for all the crystals of this family containing praseodymium ions, the temperature evolutions of the total anisotropy fields are poorly described by the Brillouin function for S = 5/2.

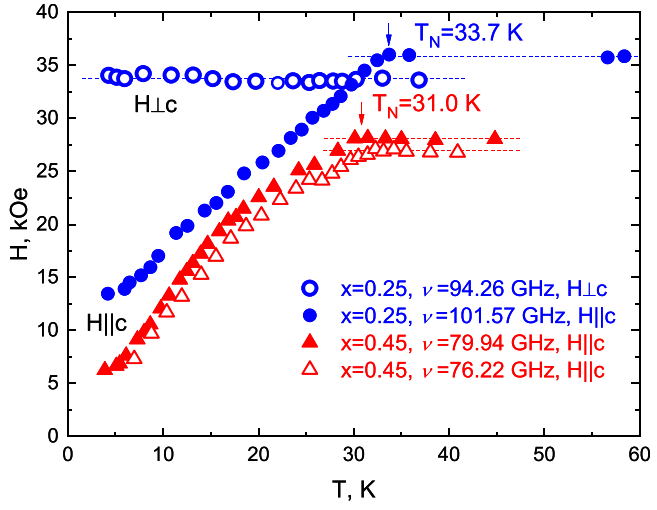

Fig. 4. Temperature dependences of the resonance fields (AFMR) in the crystals with x = 0.25 (for ***H*||*c*** and ***H*⊥*c***) and x = 0.45 (for ***H*||*c***).

3.3. AFMR in the $Pr_xY_{1-x}Fe_3(BO_3)_4$ crystal with $x = 0.67$

In accordance with the powder neutron investigation [21], the most active transformation from the EP to EA antiferromagnetic structure occurs in the range of the Pr-content x = 0.55÷0.67. In this range, the inclination angle between the antiferromagnetic vector and the crystal c-axis at T = 1.5 K changes from 63° to 23°. Thus, the crystal with x = 0.67 is of particular interest for resonance studies. Its antiferromagnetic structure is already close to the EA structure of $PrFe_3(BO_3)_4$, and it would be reasonable to expect the resonant properties to be similar to AFMR for the EA antiferromagnet. In fact, in the low fields applied at T = 4.2 K along the trigonal axis of the crystal, one can observe typical frequency-field dependences 1 and 1′(Fig. 6), which are linearly dependent on the field, these being described by Eq. (1) with the parameters given in Table 1. The expected field of the spin-flop transition $H_{sf} \approx H_{C2}$ = 19.8 kOe at T = 4.2 K corresponds to the obtained value of the energy gap H_Δ in the AFMR spectrum. Above this field in the spin-flop phase, a frequency-field dependence of AFMR was expected to be observed which is close to oscillation branch 2, shown in Fig. 6 by the dashed line. However, in

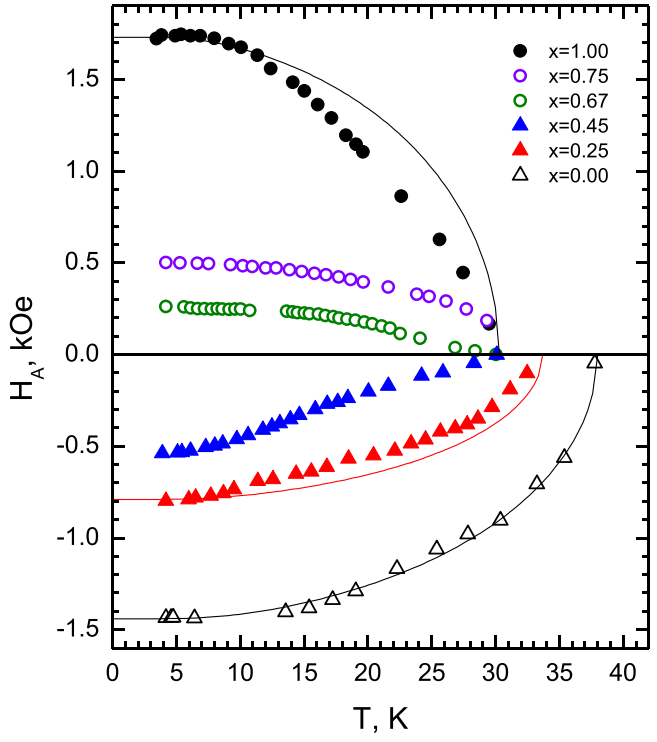

Fig. 5. Temperature dependences of the total anisotropy for the crystals $Pr_xY_{1-x}Fe_3(BO_3)_4$; solid lines – Brillouin functions for S= 5/2.

fact, oscillation branches 1 and 1′ are observed only up to some critical field $H_c \approx 12$ kOe, which is far lower than the expected field of the spin-flop transition. Above this field, instead of branches 1 and 1′ or branch 2, there appears branch 3, shown in Fig. 6 by the red circles. The frequency-field dependence for this branch is typical for the EP antiferromagnet magnetized along the trigonal axis of the crystal and it is well described by Eq. (4) with the value of the gap being considerably lower than the one in the initial state (see Table 1).

In [21,22] the field dependences of magnetization were given for the $Pr_{0.67}Y_{0.33}Fe_3(BO_3)_4$ single crystal, measured at T= 2 K in the magnetic field applied along the trigonal axis. Indeed, on this dependence in the field H≈ 12 kOe, a magnetization jump was observed (see Fig. 6b) which was interpreted in these studies as a spin-flop transition. However, the resonance data obtained in the present study indicate that in the $Pr_{0.67}Y_{0.33}Fe_3(BO_3)_4$ crystal, upon reaching the critical field H_c, the sign of the effective field of the total magnetic anisotropy changes, which results in the spin reorientation transition from the EA to the EP state and in the jump of magnetization in Fig. 6b.

The difference between these types of transitions is in the following. For the spin-flop transition, it is typical that the EA antiferromagnet in the spin-flop phase at $H > H_c$ does remain the EA one, and the loss in the anisotropic energy in this case is compensated by the gain in Zeeman energy due to the difference in the magnetic susceptibilities ($\chi_\perp - \chi_\parallel$). The spin reorientation transition occurring in the $Pr_{0.67}Y_{0.33}Fe_3(BO_3)_4$ crystal, has another physical nature: one of the contributions into the total magnetic anisotropy (apparently, from the RE subsystem) depends on the applied magnetic field, with the competing contributions from the RE and iron subsystems in this crystal being close in the absolute values. Thus, at some critical value of the external magnetic field, the total field of the resulting anisotropy changes its sign. A possible reason for this anisotropy dependence is discussed in Section 4.

It is worth noting that anomalies in the resonance spectrum were also observed at the magnetic field corresponding to the critical field

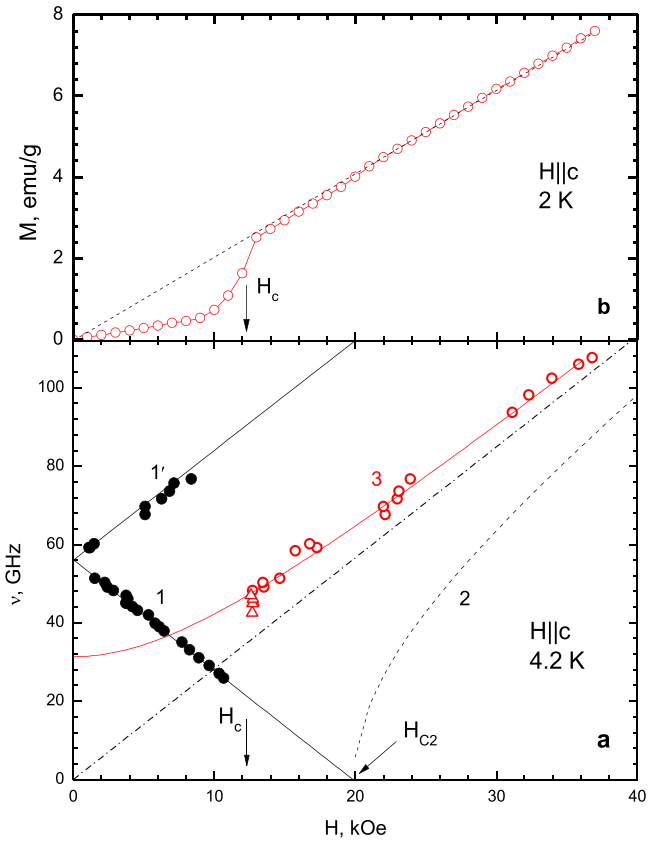

Fig. 6. a - frequency-field dependences of AFMR in $Pr_{0.67}Y_{0.33}Fe_3(BO_3)_4$ at T = 4.2 K, **H**||***c***; b – magnetization as a function of the magnetic field **H**||***c*** at T = 2 K [21].

of the transition EA→EP. These anomalies are due to a change in the microwave signal, reflected from the short-circuited waveguide with the sample, in which the spin reorientation transition occurs. The location of this anomaly does not depend on the measurement frequency; it is a non-resonant response to the transition EA→EP. On the frequency-field dependence (Fig. 6) some points of this response are indicated by the triangles.

The temperature dependences of the resonance fields for the EA and EP states measured at a frequency of 51.32 GHz are given in Fig. 7a. As in the case of the pure $PrFe_3(BO_3)_4$, for the oscillations in the EA state (open circles), the resonance field, corresponding to descending branch (1), first decreases upon the crystal heating, then, with the transition to ascending branch (1) at T≈ 10 K increases with the further heating. In the paramagnetic state above $T_N = 30.4$ K, the resonance field is independent of the temperature. Based on these data, the effective anisotropy field calculated as a function of the temperature is shown in Fig. 5. As in the case with x = 0.25 and 0.45, this temperature dependence is also poorly described by the Brillouin function.

Of special interest is the temperature dependence of the resonance field for the magnetic field induced EP state (the open blue triangles for the frequency of 51.32 GHz in Fig. 7a). Upon heating the crystal, the resonance field increases, which is indicative of the energy gap decrease for this state with the heating. This increase of the resonance field persists up to about 20 K, and upon reaching this temperature the resonance line gradually disappears. Fig. 7b shows the temperature evolution of the resonance spectrum for the EP phase upon approaching the temperature of 20 K. The spectrum measured at 13.8 K is a symmetric resonance line about 2.5 kOe wide. A wave-like anomaly is observed to the left of the line in the lower fields, representing the non-resonant microwave response to the EA→EP transition. As in the static measurements [22], this

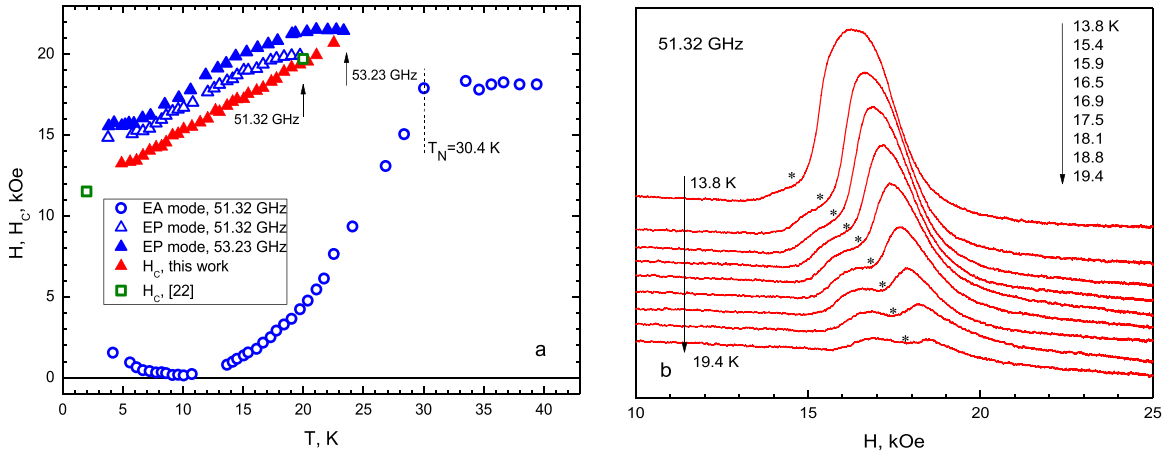

Fig. 7. a - temperature dependences of the resonance fields and critical field of the EA→EP transition in the single crystal with x = 0.67; b - temperature evolution of the EP phase resonance spectrum.

transition is extended in a certain field range, the center of the transition region being marked with an asterisk. With an increase in the temperature, the critical field of the transition increases, its temperature dependence being shown in Fig. 7a by the red triangles. Approaching T ≈ 20 K, the critical field overtakes the resonance line, which gradually disappears. Thus, the disappearance of the resonance absorption corresponding to the induced EP state is due to the fact that the resonance field for this state at a frequency of 51.32 GHz becomes smaller than the critical field of the transition to the EP state at a certain temperature which is marked with an arrow in the Figure. Fig. 7a also shows the temperature dependence of the resonance field for a similar branch of the EP state, measured at a frequency of 53.23 GHz. Since this frequency corresponds to higher resonance fields, the resonance absorption also disappears at a higher temperature T ≈ 24 K, which is also indicated with an arrow.

The points obtained from the magnetization measurements [22] at temperatures of 2 and 20 K (light green squares) are also indicated on the temperature dependence of the critical field. The magnetization data are in good agreement with the data of resonance measurements. The temperature dependence of the critical transition field is a boundary separating the states in the "magnetic field - temperature" phase diagram. The EA state is located below this boundary while above it is the field-induced EP phase.

3.4. AFMR in the $Pr_xY_{1-x}Fe_3(BO_3)_4$ crystal with $x = 0.75$

No neutron studies of the magnetic structure of this crystal have been carried out. It was assumed in [22], that the antiferromagnetic vector coincided with the trigonal axis of the crystal or deviated from the axis at a very small angle. The magnetization data [22] showed that, in terms of the magnetic properties, this composition was, indeed, the closest to pure $PrFe_3(BO_3)_4$. In the studied sample of this composition, when the magnetic field was oriented along the trigonal axis at T = 4.2 K, two jumps of magnetization were found in the magnetic fields $H_{C1} \approx 22$ kOe and $H_{C2} \approx 29$ kOe on the field dependence of the magnetization. In [22], such a two-step field dependence was interpreted as a spin-flop transition occurring through the formation of an interjacent inclined phase in the magnetic field range between the H_{C1} and H_{C2}.

The resonant properties were studied on the same sample (Sample 1) where the magnetic properties were measured [22]. The frequency-field dependences of AFMR of this sample, measured at T = 4.2 K in the magnetic field applied along the trigonal axis of the crystal, are shown in Fig. 8a. As is seen, there are two groups of dependences with different energy gaps: ~75 GHz (blue dots) and ~94 GHz (red dots). Each of these groups has a shape characteristic

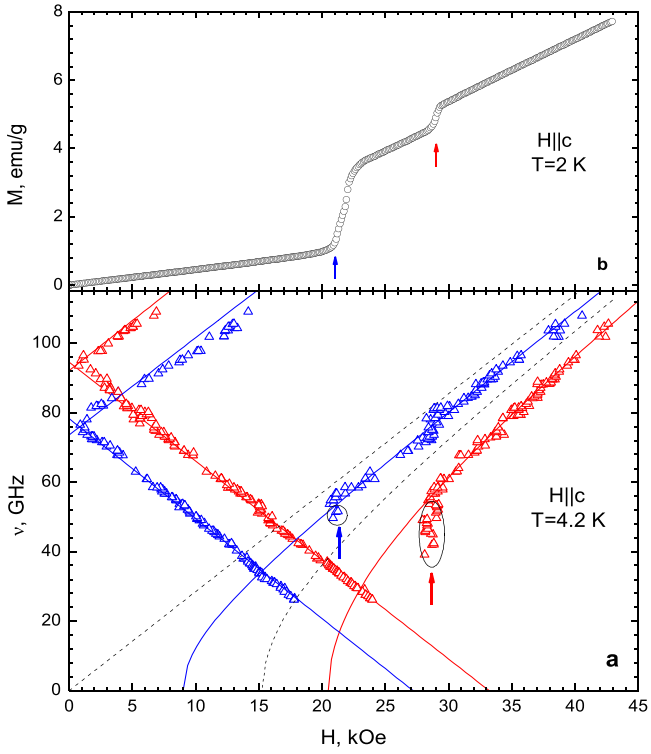

Fig. 8. a - AFMR frequency-field dependences in the crystal $Pr_{0.75}Y_{0.25}Fe_3(BO_3)_4$ (Sample 1), measured at T = 4.2 K in the magnetic field H||c; b – magnetization as a function of the magnetic field **H**||***c*** at T = 2 K.

of the EA antiferromagnet. The existence of two groups of frequency-field dependences of AFMR with different gaps suggests that the studied single crystal should not be homogeneous in composition. Apparently, it can be considered as consisting of at least two macroscopic regions with a different content of praseodymium. The groups of frequency-field dependences of AFMR, highlighted by different colors, refer to the crystal regions with different values of the effective anisotropy fields. In the area of the fields indicated by the arrows in Fig. 8a, for each group of dependences, spectrum anomalies are observed in the magnetic field, which are independent of frequency. Obviously, just as in the sample with x = 0.67, these anomalies are a non-resonant response to the spin reorientation transitions occurring in the crystal in the corresponding magnetic fields. These fields coincide with the fields at

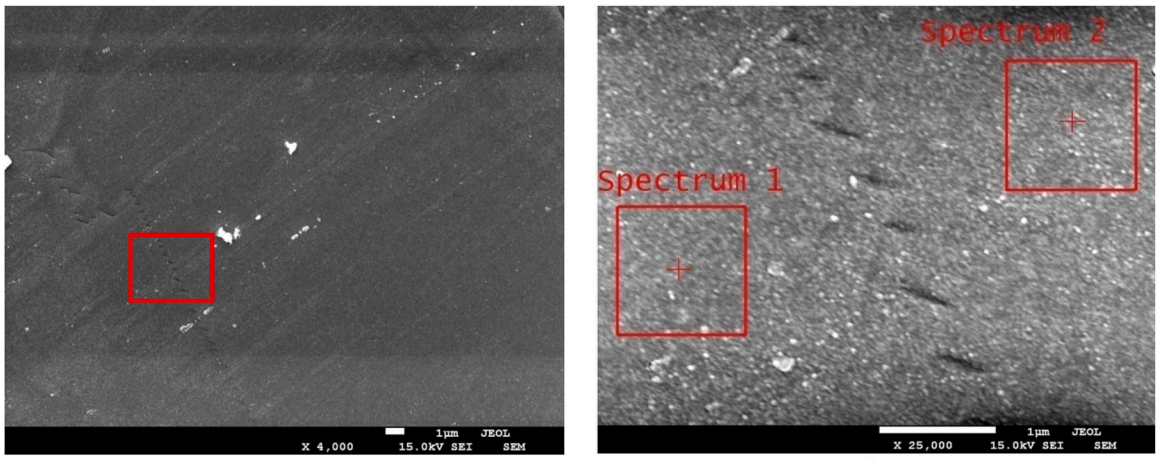

Fig. 9. SEM images of the $Pr_{0.75}Y_{0.25}Fe_3(BO_3)_4$ crystal at low (a) and middle (b) magnification.

which jumps were observed in the study of the field dependences of magnetization (see Fig. 8b) [22]. Thus, analyzing the resonant properties of Sample 1 makes it possible to interpret these jumps in magnetization as spin-flop transitions in different regions of the sample with different concentrations of praseodymium.

It should be noted that judging by the resonant properties and field dependences of the magnetization, a nonuniform distribution of praseodymium was also observed in a number of other diamagnetically dilute crystals of this family, and on one of the samples with x = 0.75, the field dependence of magnetization showed even three distinct jumps. Similar field dependences with two or even three magnetization jumps were also observed in other RE ferroborate crystals with mixed RE subsystems. In particular, multistep magnetization curves were found in crystals with mixed Ho-Nd [32] and Nd-Dy [33] subsystems. In all these studies, such a multistep character of magnetization was also associated with the formation of interjacent inclined magnetic structures. However, the results obtained in our research suggest that in the case of other substitutions in the RE subsystem, the most probable cause of such multistep magnetization curves is the nonuniform distribution of substituting ions in the crystals.

To prove the multiphase composition of Sample 1, electron microscopy studies of the $Pr_{0.75}Y_{0.25}Fe_3(BO_3)_4$ crystal surface were carried out, and the real Pr-Y concentration ratio was estimated using energy-dispersive X-ray spectroscopy. Note that the measurements were made on the same Sample 1 where the static magnetic and resonant properties were studied. Fig. 9a shows an electron microscopic image of the surface of one of the faces of the $Pr_{0.75}Y_{0.25}Fe_3(BO_3)_4$ crystal. In the lower-left part of the SEM image (see Fig. 9a), there is a clear boundary between the two regions. This boundary represents etch pits which appeared in the area of a screw dislocation formed during the crystal growth. The red rectangle (see Fig. 9a) marks the area shown in Fig. 9b at high magnification. The study of the local elemental composition of the sample shows that the proportion of praseodymium and yttrium in the regions to the left and to the right of the boundary (see Fig. 9b) is different. Table 2 shows the local elemental composition of the areas presented in Fig. 9b.

Thus, the EDS analysis evidences that two regions can actually be distinguished in the sample with the praseodymium concentration in a charge x = 0.75, where the real content of praseodymium amounts to x = 0.67 and x = 0.74.

We also studied AFMR on another sample (Sample 2) of this composition obtained by the same synthesis as the one used for the previous Sample 1. Fig. 10 shows the AFMR spectra for these two samples measured at close frequencies at T = 4.2 K in the magnetic field H||c. The spectrum for Sample 1, which is in full accordance with Fig. 8, shows two groups of lines, marked with the blue and red arrows, corresponding to the frequency-field dependences of AFMR in different regions of Sample 1. However the AFMR spectrum of Sample 2 contains only the lines close to those observed in the regions with a lower real content x = 0.67 in Sample 1. In the same spectrum, the black arrow marks the non-resonant response corresponding to the spin-flop transition in Sample 2. The frequency-field dependences of AFMR for Sample 2 completely coincide with those for Sample 1 shown in Fig. 8 by the blue triangles.

Based on the temperature evolution of the resonance field in Sample 2 measured at a frequency of 46.12 GHz in the magnetic field H||c (blue points in Fig. 11), the temperature dependence of the total anisotropy field for this sample was calculated, this being also shown in Fig. 5. The critical field of the spin-flop transition shown in Fig. 11 by the red triangles is a phase boundary separating the collinear and spin-flop states.

4. Discussion. Magnetic anisotropy in $Pr_xY_{1-x}Fe_3(BO_3)_4$

When studying the resonant properties of pure $PrFe_3(BO_3)_4$, an experimental value was obtained for the lability interval $H_{C2}-H_{C1}$ = 5.4 kOe, which significantly exceeds the value ~120 Oe predicted by the theory for a simple two-sublattice antiferromagnet, whose anisotropic properties were described by a single anisotropy constant [27]. Such a large lability interval and a significant overlap of the states below and above the spin-flop transition result in the resonance absorption being observed in the transition region only at frequencies above 70 GHz. A close value of the lability interval for this crystal was obtained in [26]. The authors in [26] believe such a

Table 2
Local elemental composition of the $Pr_{0.75}Y_{0.25}Fe_3(BO_3)_4$ sample, the data are not normalized.

	Pr (at%)	Y (at%)	Fe (at%)	B (at%)	O (at%)	Atomic proportion
Spectrum 1	3.19	1.60	14.13	9.98	67.40	$Pr_{0.67}Y_{0.33}Fe_3(BO_3)_4$
Spectrum 2	3.55	1.27	14.20	11.27	66.21	$Pr_{0.74}Y_{0.26}Fe_3(BO_3)_4$

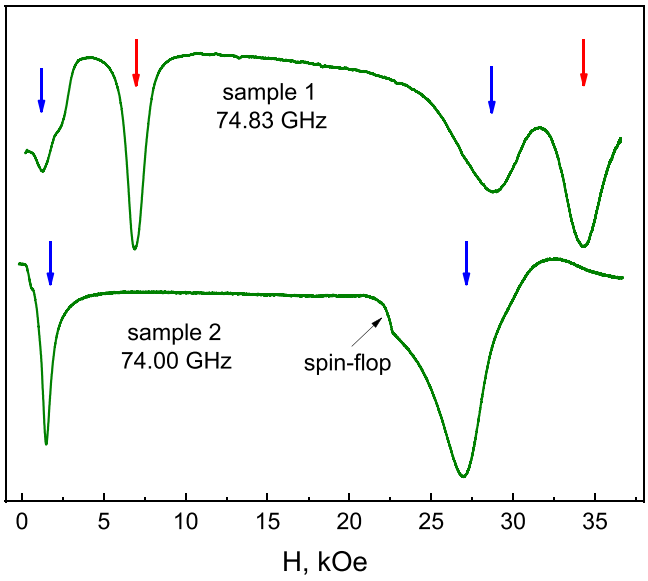

Fig. 10. AFMR spectra for the crystals with x = 0.75 (in a charge), measured at T= 4.2 K at frequencies: 74.83 GHz (Sample 1) and 74.00 GHz (Sample 2), H||c.

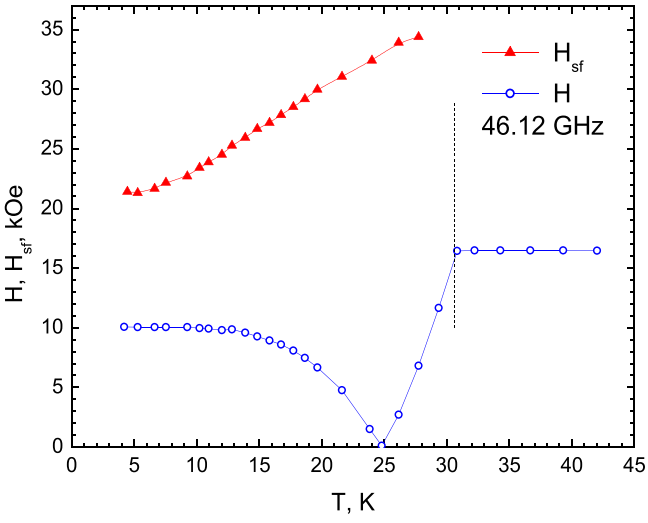

Fig. 11. Temperature dependences of the resonance field H and spin-flop transition field H_{sf}, measured in Sample 2 at 46.12 GHz, H||c.

strong difference with the theoretical prediction to be due to the fact that the contributions to the total magnetic anisotropy of the crystal from the rare-earth subsystem differ in the collinear and spin-flop states.

A significant increase in the lability interval was found upon the diamagnetic dilution of the RE subsystem. In the sample with x = 0.75, these intervals are 18 kOe and 13 kOe (Fig. 8) for the regions of the crystal with a lower and higher content of praseodymium, respectively. In other words, the closer the crystal is to the state of the mutual compensation of the Fe- and Pr-contributions to the anisotropy and the lower is the total anisotropy of the EA state, the larger is the lability interval.

In addition to the difference in the magnetic anisotropy of praseodymium in the states below and above the spin-flop transition, another reason for the appearance of a significant lability range is also possible. It is shown in [28,34] that taking into account the second anisotropy constant for the Fe^{3+} ion leads to a large overlap interval of the collinear and spin-flop states in hematite α-Fe_2O_3. In our case, the situation is more complicated due to the presence of the additional magnetic subsystem of Pr^{3+} ions. In [21,22], when analyzing the temperature and field dependences of magnetization, the magnetic anisotropy of the $Pr_xY_{1-x}Fe_3(BO_3)_4$ crystals were described as an additive sum of the contributions of the Pr- and Fe-subsystems. In this case, the contribution of the Pr-subsystem was calculated in the crystal field model, and when processing the experimental results, this contribution can be taken into account using the effective field H_A^{Pr}. The same method can be used when considering the dynamic properties of the crystal. It is shown in [25,35] that if the characteristic oscillation frequencies of the RE subsystem significantly exceed the AFMR frequencies of the iron subsystem ω^{Fe}, then it can be assumed that the dynamic variables of the RE subsystem at frequencies of the order of ω^{Fe} immediately follow the magnetic moments of the iron subsystem. The oscillation frequencies, in this case, are determined by the iron subsystem, while the magnetic anisotropy, which determines the resonant frequencies, can be described by the effective anisotropy field, which includes the contribution of both subsystems.

The magnetic anisotropy of iron ions can be considered within the framework of the phenomenological approach, in which the magnetic anisotropy energy is written as

$$\mathcal{H}_A^{Fe} = -\frac{1}{2}K_1 l_z^2 - \frac{1}{2}K_2 l_z^4, \tag{5}$$

where K_1 and K_2 are the first and the second anisotropy constants, l_z is the component of the antiferromagnetic vector in the direction of the trigonal axis. The contribution of this subsystem to the total anisotropy can be written as a sum of the corresponding first and second effective anisotropy fields $H_{A1}^{Fe} = K_1/M_0$ and $H_{A2}^{Fe} = K_2/M_0$, with M_0 being the magnetization of the antiferromagnetic sublattices in the subsystem of the Fe^{3+} ions.

Taking into account the contributions of the praseodymium subsystem and two anisotropy constants of the iron subsystem, the expressions for the critical fields H_{C1} and H_{C2} that determine the boundaries of the lability interval [28,34], take the following form:

$$H_{C1}^2 = 2H_E(H_{Asf}^{Pr} + H_{A1}^{Fe});$$
$$H_{C2}^2 = 2H_E(H_A^{Pr} + H_{A1}^{Fe} + H_{A2}^{Fe}). \tag{6}$$

The frequency softening of the descending branch of oscillations in the collinear region occurs in the critical field H_{C2}, while that of the spin-flop mode is observed in the field H_{C1}. Expressions (6) take into account that the anisotropy fields of the praseodymium subsystem in the collinear state H_A^{Pr} and in the spin-flop state H_{Asf}^{Pr} may not coincide in the general case.

One can see from expressions (6) that the large lability interval can be due both to the contribution of the second anisotropy constant into the iron subsystem and to the difference in the effective anisotropy fields of the praseodymium subsystem in the collinear and spin-flop states.

For further analysis of the magnetic anisotropy in the $Pr_xY_{1-x}Fe_3(BO_3)_4$ crystals, we assume that the magnetic anisotropy of the iron subsystem does not experience significant changes upon the diamagnetic dilution of the praseodymium subsystem. This makes it possible to independently determine the field H_{A1}^{Fe} from the resonance studies of $YFe_3(BO_3)_4$ [10] since it is known that the gap in the spectrum for the high-frequency branch of oscillations of the EP antiferromagnet is determined only by the first anisotropy constant [36]. Therefore, the effective anisotropy field measured at T= 4.2 K in [10] is $H_{A1}^{Fe} = -1.44$ kOe.

Consider in more detail the anisotropic properties of $PrFe_3(BO_3)_4$. The values of the critical fields H_{C1} = 43.91 kOe and H_{C2} = 49.17 kOe at T= 4.2 K do not allow one to independently calculate the remaining three parameters H_A^{Pr}, H_{Asf}^{Pr}, and H_{A2}^{Fe}. Therefore, to begin with, we assume that the effective anisotropy field for the praseodymium subsystem does not change upon the spin-flop transition, $H_A^{Pr} = H_{Asf}^{Pr}$.

In this case, the overlap interval of the collinear and spin-flop states is determined only by the second anisotropy field of the iron subsystem:

$$\delta H_{lab} = H_{C2}^2 - H_{C1}^2 = 2H_E H_{A2}^{Fe} \quad (7)$$

Hence, for T = 4.2 K one finds the value of the effective field determined by the second anisotropy constant, H_{A2}^{Fe}=0.35 kOe, and the anisotropy field of the praseodymium subsystem $H_A^{Pr} = H_{Asf}^{Pr}$= 2.82 kOe. The second anisotropy constant of the iron subsystem turns out to be positive, in contrast to the first one, and only in this case, the state overlap condition is satisfied $H_{C2} > H_{C1}$.

The obtained values of the anisotropy fields for the iron subsystem can be used to find the anisotropy field H_A^{Pr} in the crystal with x = 0.75. From the resonance data for the collinear state of this composition in Fig. 8a (blue dots) it follows that the critical field H_{C2} at T = 4.2 K amounts to H_{C2} = 20.5 kOe. Hence, one obtains H_A^{Pr}=1.61 kOe. However, based on the condition $H_A^{Pr} = H_{Asf}^{Pr}$, then the critical field for the spin-flop state should be H_{C1} = 15.82 kOe. The corresponding theoretical frequency-field dependence for the spin-flop resonance mode, shown in Fig. 8a by the dotted line, differs significantly from the experimental one, and the calculated value of the critical field H_{C1} significantly exceeds the experimentally measured value H_{C1} = 9.0 kOe. The reason for this discrepancy is that even if we assume that in pure $PrFe_3(BO_3)_4$ the condition $H_A^{Pr} = H_{Asf}^{Pr}$ is satisfied, then in the diluted crystal a significant part of the lability interval is due to the difference in the anisotropy fields of the praseodymium subsystem in the collinear and spin-flop states. Based on the experimental value of H_{C1} and the value of H_{A2}^{Fe}=0.35 kOe, then in the spin-flop state the effective anisotropy field of the praseodymium subsystem amounts to H_{Asf}^{Pr}=1,5 kOe at T= 4.2 K.

Similar calculations for another phase of this crystal with a higher content of Pr ions also show that the large overlap interval of states cannot be accounted for only by the contribution of the second anisotropy field of the iron subsystem. The calculations give the following values of the effective anisotropy fields of the praseodymium subsystem at T= 4.2 K: H_A^{Pr}=1.88 kOe and H_{Asf}^{Pr}=1.74 kOe.

Thus, it has to be recognized that the large lability interval both in pure $PrFe_3(BO_3)_4$ and in the crystals with the diamagnetically diluted praseodymium subsystem cannot be explained only by the contribution of the second iron anisotropy field. It is also necessary to take into account the difference in the praseodymium anisotropy fields in the states above and below the reorientation transition. Consequently, the value of H_{A2}^{Fe}=0.35 kOe, which was obtained without taking this difference into account, is overestimated, and the values of the effective anisotropy fields of praseodymium calculated with this value in mind are incorrect. The permissible upper limit of the effective field H_{A2}^{Fe} can be found through the analysis of the anisotropic properties of the crystal with x = 0.67. In this crystal, the energy gap ω_c^{EP}= 31.41 GHz measured in the magnetic field-induced EP phase at T = 4.2 K is determined only by the contributions of praseodymium and the first iron anisotropy constant; thus, one has:

$$H'_A = H_{AEP}^{Pr} + H_{A1}^{Fe} = -0.09 \text{ kOe}.$$

However, the induced EP state is determined by the total anisotropy field, which also includes the contribution of the second iron anisotropy constant, this total field being negative:

$$H_A = H_{AEP}^{Pr} + H_{A1}^{Fe} + H_{A2}^{Fe} < 0,$$

Hence, one obtains the upper limit for the second anisotropy field of iron:

$$H_{A2}^{Fe} < 0.09 \text{ kOe}. \quad (8)$$

Based on this upper limit, it is possible to estimate the admissible portion of the lability interval, which may be due to the contribution of the second iron anisotropy constant. From expression (7) one obtains that this portion does not exceed δH_{lab} < 1.3 kOe and δH_{lab} < 2.5 kOe for x = 1 and x = 0.75, respectively. Consequently, the main contribution to this interval is made by the difference between the anisotropic contributions of praseodymium in the states below and above the spin-flop transition.

Since the absolute value of the second iron anisotropy field H_{A2}^{Fe} does not exceed 6% of the value of the first iron anisotropy field, an average value H_{A2}^{Fe} = 0.04kOe can be set to estimate the anisotropic contribution of praseodymium; in this case, the absolute error in estimating the praseodymium anisotropy field will not exceed this value. Table 1 shows the values of the praseodymium anisotropy fields calculated from the energy gaps at T = 4.2 K, given that for the entire family of $Pr_xY_{1-x}Fe_3(BO_3)_4$ crystals the following holds:

$$H_{A1}^{Fe} = -1.44 \text{ kOe and } H_{A2}^{Fe} = (0.04 \pm 0.04) \text{ kOe}.$$

The values of the praseodymium anisotropy fields for the field-induced EP or spin-flop states are also given there. For the EP state of the crystal with x = 0.67, this value was calculated from the energy gap for the EP state, and for the spin-flop states in the crystals with x = 1.0 and 0.75 from the corresponding values of the critical fields H_{C1}. One can note a significant (up to 20%) decrease in the praseodymium anisotropy field in the states induced by an external magnetic field compared to the initial phase.

Fig. 12 shows the concentration dependences of the total anisotropy field and the contribution of the praseodymium subsystem at T = 4.2 K. Note that both fields depend almost linearly on the praseodymium concentration.

Thus, the analysis of the anisotropic properties of $Pr_xY_{1-x}Fe_3(BO_3)_4$ shows that in some crystals of this family the anisotropic contribution of praseodymium to the total crystal anisotropy field depends either on the applied magnetic field (as in the case with x = 0.67), or on the state – below or above the spin-flop transition – of the crystal (x = 0.75 ÷ 1.0). One can give the following qualitative explanation of the effect of these factors on the magnetic anisotropy of the praseodymium subsystem. The magnetic anisotropy of any RE ion can be described by the crystal field model. In the magnetically ordered state, the level splitting of the ground multiplet of the Pr^{3+} ion depends on the interaction of the ion with the

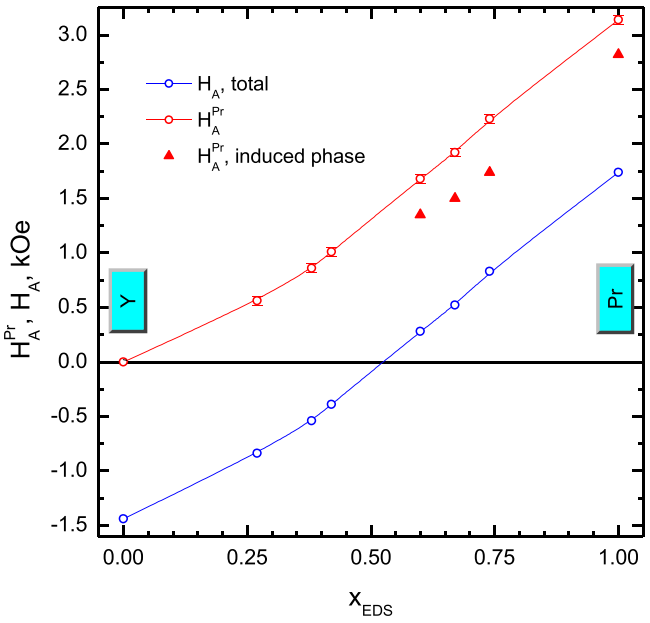

Fig. 12. Concentration dependences of the resulting anisotropy fields (blue circles), anisotropy fields of Pr in the low-field (red circles) and field-induced (red triangles) states.

effective field $\mathbf{H}_{eff} = \mathbf{H}+\mathbf{H}_{fd}$, $\mathbf{H}^i_{fd} = \lambda\mathbf{M}^{Fe}_i$ [37]. Thus, the applied magnetic field, along with the effective exchange field H_{fd}, can directly affect the change in the parameters of the crystal field. Of course, such an effect is much weaker due to the fact that $H << H_{fd}$. However, in the region of the formation of the inclined magnetic structure, when there is almost complete mutual compensation of the contributions of the iron and praseodymium subsystems, even a relatively weak magnetic field can have a noticeable effect on the value and even sign of the total anisotropy field. Similar magnetic field-induced EA→EP transitions were observed in the crystals $GdFe_3(BO_3)_4$ [10,15] and $HoFe_3(BO_3)_4$ [14], in which the anisotropic contributions of the RE and iron subsystems are also close to mutual compensation. In addition, it should be kept in mind that upon the spin-flop transition, the vector of the effective exchange field $\mathbf{H}_{fd}$ acting on the Pr ions from the iron subsystem changes its orientation abruptly. Apparently, this can also lead to changes in the magnetic anisotropy of the praseodymium subsystem in the spin-flop state.

To find the real ratio of the Pr-Y concentrations, we also carried out energy dispersive spectroscopy studies of the crystal surfaces of all the $Pr_xY_{1-x}Fe_3(BO_3)_4$ samples with the diamagnetically diluted praseodymium subsystem. In most samples, the actual content of Pr turned out to be 85÷90% of the one in the charge. The exception is the sample with x = 0.25 with the maximal yttrium dilution among the studied samples, in which the actual content turned out to be 8% higher than the one in the charge. The actual concentrations of praseodymium are given for all the samples in a separate column of Table 1. In this article, for convenience of comparison with the results of our previous studies [21,22], we retained the labeling of the samples in accordance with the content in the charge, and only the concentration dependence of the anisotropy fields in Fig. 12 is given, depending on the actual content of praseodymium found by EDS.

5. Conclusion

The spin dynamics of the $Pr_xY_{1-x}Fe_3(BO_3)_4$ crystals with x = 0÷1 were studied. The results confirm the conclusions of neutron and magnetization studies that, as the praseodymium subsystem is diamagnetically diluted, the magnetic structure is transformed from the easy axis to easy plane one. The temperature dependences of the effective anisotropy fields, determining the gap of the AFMR spectrum, were studied.

In the $Pr_xY_{1-x}Fe_3(BO_3)_4$ crystals with x = 0.75 and x = 1, a large lability interval was found with the coexistence of the collinear and spin-flop states. It is shown that the existence of such an interval can be accounted for by the joint action of the second anisotropy constant of the iron subsystem and by the difference in the effective anisotropy fields of praseodymium in the collinear and spin-flop states, with the latter contribution being dominant.

In the $Pr_{0.67}Y_{0.23}Fe_3(BO_3)$ crystal, the magnetic field applied along the trigonal axis of the crystal was found to lead to an orientational transition from the EA to EP state. A magnetic phase diagram of states was built. The reason for the transition is assumed to be the field dependence of the effective anisotropy field of the praseodymium subsystem, which, under the conditions of almost complete mutual compensation of the contributions of the iron and praseodymium subsystems, leads to a change in the sign of the total anisotropy.

Using the resonance and electron microscopy studies, it was established that in the diamagnetically diluted crystals with a high content of praseodymium in some samples, regions with different Pr-Y concentration ratios were formed due to the inhomogeneous distribution of praseodymium. Consequently, the jumps found in the field dependences of the magnetization of these crystals are due to the spin-flop transitions sequentially occurring in the areas of the crystals with different concentrations of praseodymium.

Estimates were obtained for the contributions of the praseodymium subsystem to the total anisotropy of the crystals of this family; the concentration dependence of these effective fields turned out to be almost linear. In the crystals with x = 0.67 ÷ 1.0, a significant decrease in the effective anisotropy fields of the praseodymium subsystem in the field-induced EP and spin-flop states was found as compared to the collinear EA phase.

In the $Pr_xY_{1-x}Fe_3(BO_3)_4$ crystals, both the effective total anisotropy fields and the praseodymium anisotropic contribution depend almost linearly on the praseodymium concentration x.

CRediT authorship contribution statement

A.I. Pankrats: Conceptualization, Investigation, Writing – review & editing, Supervision. **S.M. Zharkov:** Investigation, Formal analysis, Visualization. **G.M. Zeer:** Investigation, Formal analysis. **I.A. Gudim:** Resources.

Data Availability

The datasets generated and analyzed during the current study are available from the corresponding author on reasonable request.

Declaration of Competing Interest

The authors declare that they have no known competing financial interests or personal relationships that could have appeared to influence the work reported in this paper.

Acknowledgements

The authors acknowledge the assistance of R. Mironov in some resonance measurements. The SEM and EDS investigations were conducted in the SFU Joint Scientific Center supported by the State assignment (#FSRZ-2020–0011) of the Ministry of Science and Higher Education of the Russian Federation.

Prime Novelty Statement

Experimental investigations of the spin dynamics, magnetic structures and magnetic anisotropy have been carried out in $Pr_xY_{1-x}Fe_3(BO_3)_4$ single crystals using antiferromagnetic resonance (AFMR). AFMR is very sensitive to the magnetic structure of a crystal. As opposed to powder neutron diffraction, AFMR allows investigating the magnetic structure transformation upon changing the external magnetic field. Using the AFMR study of a $Pr_{0.67}Y_{0.23}Fe_3(BO_3)$ crystal, a spin reorientation transition from the easy-axis (EA) to the easy-plane (EP) state has been found in the magnetic field applied along the trigonal axis. The reason for the transition is assumed to be the field dependence of the effective anisotropy field of the praseodymium subsystem.

The AFMR method also makes it possible to quantitatively determine the total effective field of the magnetic anisotropy, as well as to separate the contributions of the magnetic subsystems of iron and praseodymium ions to the anisotropy. In the $Pr_xY_{1-x}Fe_3(BO_3)_4$ crystals, both the effective total anisotropy fields and the praseodymium contribution depend almost linearly on the praseodymium concentration x.

In the crystals with x = 0.67 ÷ 1.0, a significant decrease in the effective anisotropy fields of the praseodymium subsystem in the field-induced EP and spin-flop states has been found as compared to the collinear EA phase.

References

[1] Y. Hinatsu, Y. Doi, K. Ito, M. Wakeshima, A. Alemi, Magnetic and calorimetric studies on rare-earth iron borates $LnFe_3(BO_3)_4$ (Ln=Y, La–Nd, Sm–Ho), J. Solid State Chem. 172 (2003) 438–445, https://doi.org/10.1016/S0022-4596(03)00028-8

[2] S.A. Klimin, D. Fausti, A. Meetsma, L.N. Bezmaternykh, P.H.M. van Loosdrecht, T.T.M. Palstra, Evidence for differentiation in the iron-helicoidal chain in $GdFe_3(BO_3)_4$, Acta Crystallogr. B 61 (2005) 481–485, https://doi.org/10.1107/S0108768105017362

[3] S.R. Chinn, H.Y.-P. Hung, CW laser action in acentric $NdAl_3(BO_3)_4$ and $KNdP_4O_{12}$, Opt. Commun. 15 (1975) 345–350, https://doi.org/10.1016/0030-4018(75)90242-4

[4] H.Y.-P. Hong, K. Dwight, Crystal structure and fluorescence lifetime of $NdAl_3(BO_3)_4$, a promising laser material, Mater. Res. Bull. 9 (1974) 1661–1665, https://doi.org/10.1016/0025-5408(74)90158-5

[5] P. Dekker, J.M. Dawes, J.A. Pipper, Y. Liu, J. Wang, 1.1 W CW self-frequency-doubled diode-pumped Yb:$YAl_3(BO_3)_4$ laser, Opt. Commun. 195 (2001) 431–436, https://doi.org/10.1016/S0030-4018(01)01347-5

[6] A.K. Zvezdin, S.S. Krotov, A.M. Kadomtseva, G.P. Vorob'ev, Yu.F. Popov, A.P. Pyatakov, L.N. Bezmaternykh, E.A. Popova, Magnetoelectric effects in gadolinium iron borate $GdFe_3(BO_3)_4$, JETP Lett. 81 (2005) 272–276, https://doi.org/10.1134/1.1931014

[7] A.K. Zvezdin, G.P. Vorob'ev, A.M. Kadomtseva, Yu.F. Popov, A.P. Pyatakov, L.N. Bezmaternykh, A.V. Kuvardin, E.A. Popova, Magnetoelectric and magnetoelastic interactions in $NdFe_3(BO_3)_4$ multiferroics, JETP Lett. 83 (2006) 509–514, https://doi.org/10.1134/S0021364006110099

[8] A.M. Kadomtseva, Yu.F. Popov, G.P. Vorob'ev, A.P. Pyatakov, S.S. Krotov, K.I. Kamilov, V.Yu Ivanov, A.A. Mukhin, A.K. Zvezdin, A.M. Kuz'menko, L.N. Bezmaternykh, I.A. Gudim, V.L. Temerov, Magnetoelectric and magnetoelastic properties of rare-earth ferroborates, Low Temp. Phys. 36 (2010) 511–521, https://doi.org/10.1063/1.3457390

[9] C. Ritter, A. Vorotynov, A. Pankrats, G. Petrakovskiĭ, V. Temerov, I. Gudim, R. Szymczak, Magnetic structure in iron borates $RFe_3(BO_3)_4$(R = Y,Ho): a neutron diffraction and magnetization study, J. Phys.: Condens. Matter 20 (2008) 365209, https://doi.org/10.1088/0953-8984/20/36/365209

[10] A.I. Pankrats, G.A. Petrakovskiĭ, L.N. Bezmaternykh, V.L. Temerov, Antiferromagnetic resonance and magnetic anisotropy in single crystals of the $YFe_3(BO_3)_4$-$GdFe_3(BO_3)_4$ system, Phys. Solid State 50 (2008) 79–83, https://doi.org/10.1134/S1063783408010150

[11] C. Ritter, A. Vorotynov, A. Pankrats, G. Petrakovskiĭ, V. Temerov, I. Gudim, R. Szymczak, Magnetic structure in iron borates $RFe_3(BO_3)_4$ (R = Er, Pr): a neutron diffraction and magnetization study, J. Phys.: Condens. Matter 22 (2010) 206002, https://doi.org/10.1088/0953-8984/22/20/206002

[12] M. Janoschek, P. Fischer, J. Schefer, B. Roessli, V. Pomjakushin, M. Meven, V. Petricek, G. Petrakovskii, L. Bezmaternykh, Single magnetic chirality in the magnetoelectric $NdFe_3(^{11}BO_3)_4$, Phys. Rev. B 81 (2010) 094429, https://doi.org/10.1103/PhysRevB.81.094429

[13] H. Mo, C.S. Nelson, L.N. Bezmaternykh, V.L. Temerov, Magnetic structure of the field-induced multiferroic $GdFe_3(BO_3)_4$, Phys. Rev. B 78 (2008) 214407, https://doi.org/10.1103/PhysRevB.78.214407

[14] A. Pankrats, G. Petrakovskii, A. Kartashev, E. Eremin, V. Temerov, Low-temperature magnetic phase diagram of $HoFe_3(BO_3)_4$ holmium ferroborate: a magnetic and heat capacity study, J. Phys.: Condens. Matter 21 (2009) 436001, https://doi.org/10.1088/0953-8984/21/43/436001

[15] A.I. Pankrats, G.A. Petrakovskii, L.N. Bezmaternykh, O.A. Bayukov, Antiferromagnetic resonance and phase diagrams of gadolinium ferroborate $GdFe_3(BO_3)$, JETP 99 (4) (2004) 766–775, https://doi.org/10.1134/1.1826168

[16] R.P. Chaudhury, F. Yen, B. Lorenz, Y.Y. Sun, L.N. Bezmaternykh, V.L. Temerov, C.W. Chu, Magnetoelectric effect and spontaneous polarization in $HoFe_3(BO_3)_4$ and $Ho_{0.5}Nd_{0.5}Fe_3(BO_3)_4$, Phys. Rev. B 80 (2009) 104424, https://doi.org/10.1103/PhysRevB.80.104424

[17] M. Platunov, N. Kazak, V. Dudnikov, V. Temerov, I. Gudim, Yu Knyazev, S. Gavrilkin, V. Dyadkin, Iu Dovgaliuk, D. Chernyshov, A. Hen, F. Wilhelm, A. Rogalev, S. Ovchinnikov, Element selective magnetism in $H_{0.5}Nd_{0.5}Fe_3(BO_3)_4$ single crystal probed with hard X-ray magnetic circular dichroism, JMMM 479 (2019) 312–316, https://doi.org/10.1016/j.jmmm.2019.02.040

[18] F. Yu, A.M. Popov, G.P. Kadomtseva, A.A. Vorob'ev, V. Mukhin, Yu, A.M. Ivanov, A.S. Kuz'menko, L.N. Prokhorov, V.L. Bezmaternykh Temerov, Observation of spontaneous spin reorientation in $Nd_{1-x}Dy_xFe_3(BO_3)_4$ ferroborates with a competitive R-Fe exchange, JETP Lett. 89 (2009) 345–351, https://doi.org/10.1134/S002136400907008X

[19] A.I. Pankrats, G.A. Petrakovskii, V.I. Tugarinov, A.V. Kartashev, V.L. Temerov, Magnetic resonance and thermophysical studies of the magnetic phase diagram for a $GdFe_{2.1}Ga_{0.9}(BO_3)_4$ single crystal, JETP 113 (2011) 483–489, https://doi.org/10.1134/S1063776111070089

[20] A.M. Kadomtseva, Yu.F. Popov, G.P. Vorob'ev, A.A. Mukhin, V.Yu Ivanov, A.M. Kuz'menko, L.N. Bezmaternykh, Influence of the ground state of the Pr^{3+} ion on magnetic and magnetoelectric properties of the $PrFe_3(BO_3)_4$ multiferroic, JETP Lett. 87 (2008) 39–44, https://doi.org/10.1134/S0021364008010104

[21] C. Ritter, A.I. Pankrats, A.A. Demidov, D.A. Velikanov, V.L. Temerov, I.A. Gudim, Inclined magnetic structure of iron borate $Pr_xY_{1-x}Fe_3(BO_3)_4$: a neutron diffraction study and crystal-field calculations, Phys. Rev. B 91 (2015) 134416, https://doi.org/10.1103/PhysRevB.91.134416

[22] A.I. Pankrats, A.A. Demidov, C. Ritter, D.A. Velikanov, S.V. Semenov, V.I. Tugarinov, V.L. Temerov, I.A. Gudim, Transformation from an easy-plane to an easy-axis antiferromagnetic structure in the mixed rare-earth ferroborates $Pr_xY_{1-x}Fe_3(BO_3)_4$: magnetic properties and crystal field calculations, J. Phys.: Condens. Matter 28 (2016) 396001, https://doi.org/10.1088/0953-8984/28/39/396001

[23] L.N. Bezmaternykh, V.L. Temerov, I.A. Gudim, N.A. Stolbovaya, Crystallization of trigonal (Tb,Er)(Fe,Ga)$_3(BO_3)_4$ phases with hantite structure in bismuth trimolybdate-based fluxes, Crystallogr. Rep. 50 (2005) S97–S99, https://doi.org/10.1134/1.2133981

[24] V.I. Tugarinov, I.Ya Makievskii, A.I. Pankrats, A computer-controlled magnetic resonance spectrometer with a pulsed magnetic field, Instrum. Exp. Tech. 47 (2004) 472–476, https://doi.org/10.1023/B:INET.0000038391.41765.c9

[25] A.M. Kuz'menko, A.A. Mukhin, V.Yu Ivanov, A.M. Kadomtseva, S.P. Lebeev, L.N. Bezmaternykh, Antiferromagnetic resonance and dielectric properties of rare-earth ferroborates in the submillimeter frequency range, JETP 113 (2011) 113, https://doi.org/10.1134/S106377611105013X

[26] A.N. Bludov, V.A. Pashchenko, M.I. Kobets, V.A. Bedarev, D.N. Merenkov, S.L. Gnatchenko, I.A. Gudim, Antiferromagnetic resonance in crystalline $PrFe_3(BO_3)_4$, Low Temp. Phys. 44 (2018) 139, https://doi.org/10.1063/1.5020909

[27] G. Gurevich, Magnetic Resonance in Ferrites and Antiferromagnets (Nauka, Moscow, 1973). In Russian.

[28] I.S. Jacobs, R.A. Beyerlein, S. Foner, J.P. Remeika, Field-induced magnetic phase transition in antiferromagnetic hematite (α-Fe_2O_3), Int. J. Magn. 1 (1971) 193–208.

[29] V. Glazkov, T. Soldatov, Yu Krasnikova, Numeric calculation of antiferromagnetic resonance frequencies for the noncollinear antiferromagnet, Appl. Magn. Reson. 47 (2016) 1069–1080, https://doi.org/10.1007/s00723-016-0825-1

[30] L.A. Prozorova, A.S. Borovik-Romanov, Antiferromagnetic resonance of manganese carbonate in strong magnetic fields, Sov. Phys. JETP 28 (1969) 910–914 ⟨http://www.jetp.ras.ru/cgi-bin/dn/e_028_05_0910.pdf⟩.

[31] L.V. Velikov, S.V. Mironov, E.S. Rudashevsky, Study of the interaction between two spin oscillation modes during antiferromagnetic resonance in the weakly ferromagnetic phase of hematite, Sov. Phys. JETP 30 (1970) 428–432 ⟨http://www.jetp.ras.ru/cgi-bin/dn/e_030_03_0428.pdf⟩.

[32] I.A. Gudim, A.A. Demidov, E.V. Eremin, D.K. Shukla, Magnetic and Magnetodielectric Properties of $Ho_{0.5}Nd_{0.5}Fe_3(BO_3)_4$, Phys. Solid State 60 (2018) 1989–1998, https://doi.org/10.1134/S1063783418100086

[33] A.A. Demidov, I.A. Gudim, E.V. Eremin, Magnetic phase transitions in $Nd_{1-x}Dy_xFe_3(BO_3)_4$ ferroborates, JETP 114 (2012) 259–272, https://doi.org/10.1134/S1063776111160023

[34] V.I. Ozhogin, V.G. Shapiro, Premature disappearance of antiferromagnetic resonances in hematite, Sov. Phys. JETP 28 (1969) 915–922 ⟨http://www.jetp.ras.ru/cgi-bin/dn/e_028_05_0915.pdf⟩.

[35] A.M. Kuz'menko, A.A. Mukhin, V.Yu. Ivanov, A.M. Kadomtseva, L.N. Bezmaternykh, Effects of the interaction between R and Fe modes of the magnetic resonance in $RFe_3(BO_3)_4$ rare-earth iron borates, JETP Lett. 94 (2011) 294–300, https://doi.org/10.1134/S0021364011160119

[36] K.S. Aleksandrov, L.N. Bezmaternykh, G.V. Kozlov, S.P. Lebedev, A.A. Mukhin, A.S. Prokhorov, Anomalies of high-frequency magnetic permeability of hematite at the Morin phase transition, Sov. Phys. JETP 65 (1987) 591–595 ⟨http://www.jetp.ras.ru/cgi-bin/dn/e_065_03_0591.pdf⟩.

[37] N.V. Kostyuchenko, A.I. Popov, A.K. Zvezdin, Features of magnetic and magnetoelectric properties of rare-earth multiferroic $PrFe_3(BO_3)_4$ with the singlet ground state, Phys. Solid State 54 (2012) 1591–1597, https://doi.org/10.1134/S1063783412080161